THE JOURNAL OF PHYSICAL CHEMISTRY Letters

Letter

Cite This: J. Phys. Chem. Lett. 2018, 9, 6215−6223

pubs.acs.org/JPCL

Conical Intersections Induced by Quantum Light: Field-Dressed Spectra from the Weak to the Ultrastrong Coupling Regimes

Tamás Szidarovszky,*[,†] Gábor J. Halász,[‡] Attila G. Császár,[†] Lorenz S. Cederbaum,[§] and Ágnes Vibók*[,∥,⊥]

[†]Laboratory of Molecular Structure and Dynamics, Institute of Chemistry, ELTE Eötvös Loránd University and MTA-ELTE Complex Chemical System Research Group, Pázmány Péter sétány 1/A, H-1117 Budapest, Hungary

[‡]Department of Information Technology, University of Debrecen, P.O. Box 400, H-4002 Debrecen, Hungary

[§]Theoretische Chemie, Physikalisch-Chemisches Institut, Universität Heidelberg, D-69120 Heidelberg, Germany

[∥]Department of Theoretical Physics, University of Debrecen, P.O. Box 400, H-4002 Debrecen, Hungary

[⊥]ELI-ALPS, ELI-HU Non-Profit Ltd., Dugonics tér 13, H-6720 Szeged, Hungary

ABSTRACT: In classical laser fields with frequencies resonant with the electronic excitation in molecules, it is by now known that conical intersections are induced by the field and are called light-induced conical intersections (LICIs). As optical cavities have become accessible, the question arises whether their quantized modes could also lead to the appearance of LICIs. A theoretical framework is formulated for the investigation of LICIs of diatomics in such quantum light. The eigenvalue spectrum of the dressed states in the cavity is studied, putting particular emphasis on the investigation of absorption spectra of the Na_2 molecule, that is, on the transitions between dressed states, measured by employing a weak probe pulse. The dependence of the spectra on the light−matter coupling strength in the cavity and on the frequency of the cavity mode is studied in detail. The computations demonstrate strong nonadiabatic effects caused by the appearing LICI.

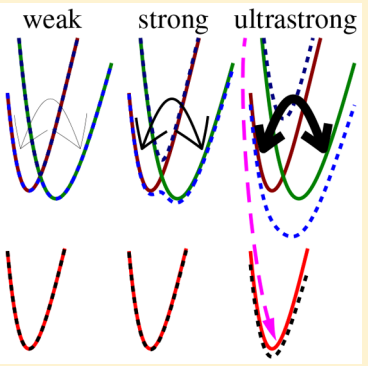

Understanding the interaction of matter with strong and ultrastrong laser pulses is a fundamental and rapidly developing field of research. With the remarkable advances in laser technology in the past few decades, it has become feasible to study this interaction experimentally.[1−3] These investigations provided insight into the strongly nonlinear domain of optical processes, associated with various unique phenomena, such as high harmonic generation,[4,5] above-threshold dissociation and ionization,[6] bond softening and hardening effects,[7−13] and light-induced conical intersections (LICIs).[14−22]

LICIs may form even in diatomic molecules when the laser light not only rotates the molecule but can also couple the vibrational with the emerging rotational degrees of freedom.[23] Theoretical and experimental studies have demonstrated that light-induced nonadiabatic effects have a significant impact on different observable dynamical properties, such as molecular alignment, dissociation probability, or angular distribution of photofragments.[14−20] Recently, signatures of light-induced nonadiabatic phenomena have been successfully identified in the classical field-dressed static rovibronic spectrum of diatomics.[24]

As an alternative to interactions of atoms or molecules with intense laser fields, strong light−matter coupling can also be achieved, both for atoms and molecules, by their confinement in microscale optical or plasmonic cavities.[25−32] Such systems are usually described in terms of field-dressed or polariton states, which are the eigenstates of the full "atom/molecule + radiation field" system. Nowadays, polaritonic chemistry is a rapidly growing field that provides a novel tool to modify and control chemical structure and dynamics. Since the pioneering experimental work by the group of Thomas Ebbesen in 2012,[33] which demonstrated that the strong light−matter coupling could modify the chemical landscapes and chemical reactions, considerable experimental[33−38] and theoretical[39−51] research activities are concentrated in this field. Among the many interesting findings, it was observed that strong coupling can modify the absorption spectrum of molecules,[34,35,39] and the formation of "supermolecular" polaritonic states leads to enhanced intermolecular nonradiative energy transfer.[36]

For atoms or molecules interacting with a cavity mode (near) resonant to an electronic transition, one usually distinguishes three regimes of field−matter coupling strengths,[26,39,52,53] as depicted in Figure 1: weak, strong, and ultrastrong. In the weak-coupling regime (see the left panel of Figure 1), the diabatic picture of photon-dressed potential energy curves (PECs) holds, and the cavity mode only couples the excited electronic state to the ground electronic state dressed by a photon. In the strong-coupling

Received: August 23, 2018
Accepted: October 8, 2018
Published: October 8, 2018

DOI: 10.1021/acs.jpclett.8b02609
J. Phys. Chem. Lett. 2018, 9, 6215−6223

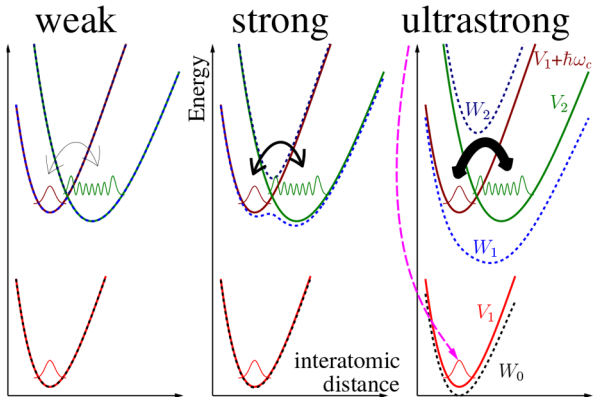

Figure 1. The three regimes of coupling strength and the related field-dressed PECs of a molecule interacting with a resonant cavity mode. The diabatic surfaces V_1 and V_2 are indicated with continuous lines, whereas the polariton surfaces W_0, W_1, and W_2 are indicated with dashed lines. $\hbar\omega_c$ is the energy of the cavity photon. The double headed arrows and the dashed red arrow represent resonant and nonresonant couplings in the cavity, respectively, see text.

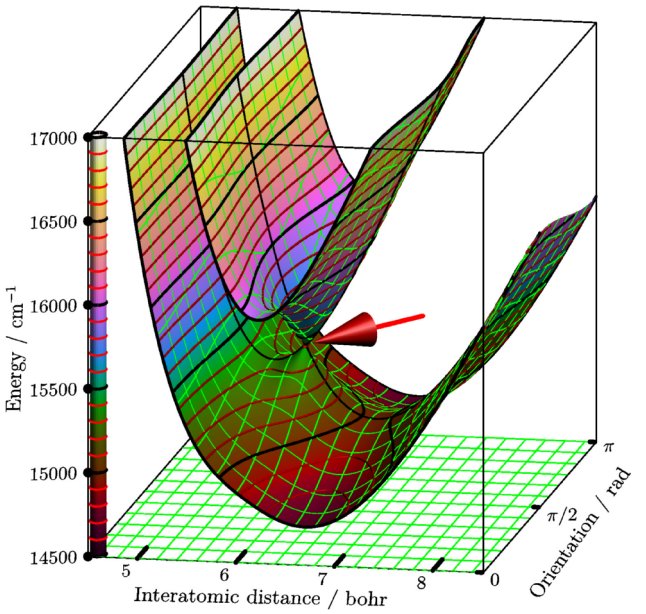

Figure 2. Two-dimensional polariton surfaces (W_1 and W_2) of the Na_2 dimer in the cavity. The one-photon coupling strength of the cavity (ε_c) corresponds to a classical field intensity of 64 GW cm^{-2}. The cavity-mode wavelength is λ_c = 653 nm. The red arrow denotes the position of the light-induced conical intersection.

regime, shown in the middle panel of Figure 1, polariton states are formed and the adiabatic picture becomes appropriate for describing the excited-state manifold, while the ground state remains essentially unchanged. Finally, in the ultrastrong-coupling regime (see the right panel of Figure 1), nonresonant couplings become strong enough to significantly modify the electronic ground state, as well.

In reality, the dashed polariton surfaces of Figure 1 are strictly valid only if the molecular axis is parallel to the preferred polarization direction of the cavity field. In contrast, when the molecular axis is perpendicular to the polarization direction of the cavity, the light−matter coupling vanishes and the diabatic picture (continuous potentials in Figure 1) is the relevant one. In fact, the orientation of a rotating molecule can change continuously between these two extremes, and the diabatic and cavity-induced polariton surfaces are continuously transformed into each other. Therefore, because of the rotation of the molecule, the upper and lower adiabatic surfaces are not completely separated but a conical intersection (CI) emerges between them (see Figure 2), at which point the nonadiabatic couplings become infinitely strong.

At the vicinity of this CI, created by the quantum light and never present in field-free diatomics, the Born−Oppenheimer picture[54,55] breaks down. The nuclear dynamics proceed on the coupled polariton surfaces, and motions along the vibrational and rotational coordinates become intricately coupled. It must be stressed that even in the case of diatomics, considering rotations completely changes the paradigm and the physical picture with respect to the description when only the vibrational, electronic, and photonic degrees of freedom are taken into account. Moreover, in contrast to field-free polyatomic molecules, where CIs are dictated by nature (they are either present or not), light-induced conical intersections in the cavity are always present between the polariton surfaces. Even for a diatomic molecule, the appropriate description needs to account for rotations, which are coupled nonadiabatically to the vibrational, electronic, and photonic modes of the system.

The purpose of the present study is to investigate the field-dressed rovibronic spectrum of diatomics in the framework of cavity quantum electrodynamics (cQED). We complement previous theoretical approaches, which mostly treated atoms or molecules in reduced dimensions or via some simplified models,[39−42,44,47−50] by accounting for all molecular degrees of freedom; that is, we treat rotational, vibrational, electronic, and photonic degrees of freedom on an equal footing. Furthermore, we incorporate for the first time the concept of LICIs with the quantized radiation field. Our work is two-fold. First, we investigate the field-dressed rovibronic spectrum of our test system, the homonuclear Na_2 molecule, to understand the effects of the cavity on the spectrum and to identify the direct signatures of a LICI created by the quantized cavity radiation field. Second, the coupling strength and cavity-mode wavelength dependence of the spectrum from the weak to the ultrastrong coupling regimes are investigated.

For simulating the weak-field absorption spectrum of molecules confined in small optical cavities, we first determine the field-dressed states, that is, the eigenstates of the full "molecule + radiation field" system; then, we compute the dipole transition amplitudes between the field-dressed states with respect to a probe pulse. We assume the probe pulse to be weak; therefore, transitions induced by it should be dominated by one-photon processes. This implies that the standard approach[56] of using first-order time-dependent perturbation theory to compute the transition amplitudes is adequate.

Within the framework of cQED and the electric dipole representation, the Hamiltonian of a molecule interacting with a single cavity mode can be written as[57]

$$\hat{H}_{\mathrm{tot}} = \hat{H}_{\mathrm{mol}} + \hat{H}_{\mathrm{rad}} + \hat{H}_{\mathrm{int}} \quad (1)$$

where $\hat{H}_{\mathrm{mol}}$ is the field-free molecular Hamiltonian, $\hat{H}_{\mathrm{rad}}$ is the radiation-field Hamiltonian, and $\hat{H}_{\mathrm{int}}$ is the interaction term

DOI: 10.1021/acs.jpclett.8b02609
J. Phys. Chem. Lett. 2018, 9, 6215−6223

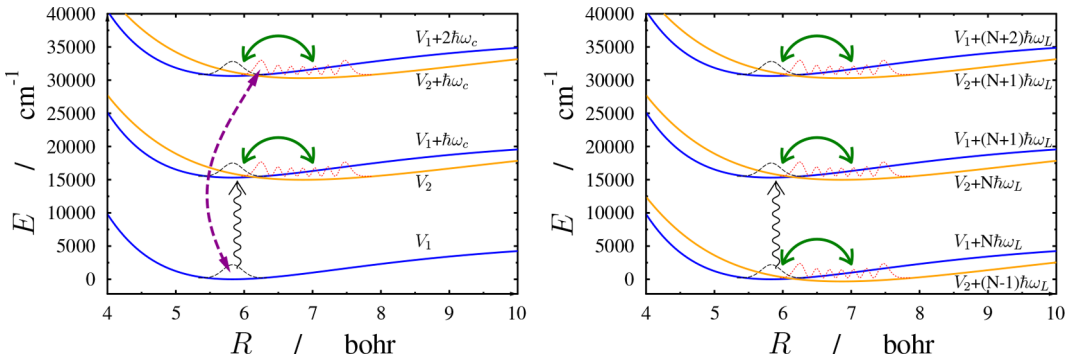

Figure 3. Arrangement of the molecular electronic states in the cavity versus those in a classical field. Left: PECs of Na_2, dressed with different number of photons of the cavity field, obtained with a dressing-light wavelength of λ = 653 nm. Vibrational probability densities are drawn for states of $|1\ 0\ 0\rangle|m\rangle$-type (dashed black lines on the $V_1(R)$ + $m\hbar\omega_c$ PECs), and for states of $|2\ 6\ 1\rangle|m\rangle$-type (dotted red lines on the $V_2(R)$ + $m\hbar\omega_c$ PECs). Couplings induced by the cavity radiation field are indicated by the two double-headed arrows. The continuous green double-headed arrow represents $|1\ v\ J\rangle|m\rangle \leftrightarrow |2\ v'\ J \pm 1\rangle|m-1\rangle$-type resonant couplings, whereas the dashed purple double-headed arrow represents $|1\ v\ J\rangle|m\rangle \leftrightarrow |2\ v'\ J \pm 1\rangle|m+1\rangle$-type nonresonant couplings. Finally, the vertical black wavy arrow indicates transitions between the two manifolds of field-dressed states, resulting from the absorption of a photon of the weak probe pulse. Right: same as left panel, but for Na_2 dressed by laser light.

between the molecular dipole moment and the electric field. For a single radiation mode and an appropriate choice of the origin[57]

$$\hat{H}_{\text{rad}} = \hbar\omega_c \hat{a}^\dagger \hat{a} \tag{2}$$

and

$$\hat{H}_{\text{int}} = -\sqrt{\frac{\hbar\omega_c}{2\epsilon_0 V}}\,\hat{\mathbf{d}}\hat{\mathbf{e}}(\hat{a}^\dagger + \hat{a}) = -\frac{\varepsilon_c}{\sqrt{2}}\hat{\mathbf{d}}\hat{\mathbf{e}}(\hat{a}^\dagger + \hat{a}) \tag{3}$$

where $\varepsilon_c = \sqrt{\hbar\omega_c/(\epsilon_0 V)}$ is the cavity one-photon field, $\hat{a}^\dagger$ and $\hat{a}$ are photon creation and annihilation operators, respectively, ω_c is the frequency of the cavity mode, $\hbar$ is Planck's constant divided by 2π, ϵ_0 is the electric constant, V is the volume of the electromagnetic mode, $\hat{\mathbf{d}}$ is the molecular dipole moment operator, and $\hat{\mathbf{e}}$ is the polarization vector of the cavity mode. In the case of homonuclear diatomic molecules having no permanent dipole, representing the Hamiltonian of eq 1 in a direct product basis composed of two field-free molecular electronic states and the Fock states of the radiation field gives the Hamiltonian

$$\hat{H} = \begin{bmatrix} \hat{T}+V_1(R) & 0 & 0 & g_{12}(R,\theta)\sqrt{2} & 0 & \cdots \\ 0 & \hat{T}+V_2(R) & g_{21}(R,\theta)\sqrt{2} & 0 & 0 & \cdots \\ 0 & g_{12}(R,\theta)\sqrt{2} & \hat{T}+V_1(R)+\hbar\omega_c & 0 & 0 & \cdots \\ g_{21}(R,\theta)\sqrt{2} & 0 & 0 & \hat{T}+V_2(R)+\hbar\omega_c & g_{21}(R,\theta)\sqrt{3} & \cdots \\ 0 & 0 & 0 & g_{12}(R,\theta)\sqrt{3} & \hat{T}+V_1(R)+2\hbar\omega_c & \cdots \\ \vdots & \vdots & \vdots & \vdots & \vdots & \ddots \end{bmatrix} \tag{4}$$

with

$$g_{ij}(R,\theta) = -\sqrt{\frac{\hbar\omega}{2\epsilon_0 V}}\,d_{ij}(R)\cos(\theta) \tag{5}$$

In eqs 4 and 5, R is the internuclear distance, $V_i(R)$ is the ith PEC, $\hat{T}$ is the nuclear kinetic energy operator, $d_{ij}(R)$ is the transition dipole moment matrix element between the ith and jth electronic states, and θ is the angle between the electric field polarization vector and the transition dipole vector, assumed to be parallel to the molecular axis. For all coupling strengths investigated during this study, numerical convergence was achieved by limiting the cavity photon number to two, that is, by using the upper-left six-by-six block of the Hamiltonian of eq 4.

The $|\Psi_i^{\text{FD}}\rangle$ field-dressed states, that is, the eigenstates of the Hamiltonian of eq 1

$$\hat{H}_{\text{tot}}|\Psi_i^{\text{FD}}\rangle = E_i^{\text{FD}}|\Psi_i^{\text{FD}}\rangle \tag{6}$$

are obtained by diagonalizing the Hamiltonian of eq 4 in the basis of field-free rovibrational states. Then, the field-dressed states can be expressed as the linear combination of products of field-free molecular rovibronic states and Fock states of the dressing field, that is

$$\begin{aligned} |\Psi_i^{\text{FD}}\rangle &= \sum_{J,v,\alpha,N} C_{i,\alpha vJN}|\alpha vJ\rangle|N\rangle \\ &= \sum_{J,v,N} C_{i,1vJN}|1vJ\rangle|N\rangle + \sum_{J,v,N} C_{i,2vJN}|2vJ\rangle|N\rangle \end{aligned} \tag{7}$$

where $|jvJ\rangle$ is a field-free rovibronic state, in which the molecule is in the jth electronic, vth vibrational, and Jth rotational state, $|N\rangle$ is a Fock state of the dressing field with photon number N, and $C_{i,jvJN}$ are expansion coefficients

DOI: 10.1021/acs.jpclett.8b02609
J. Phys. Chem. Lett. 2018, 9, 6215−6223

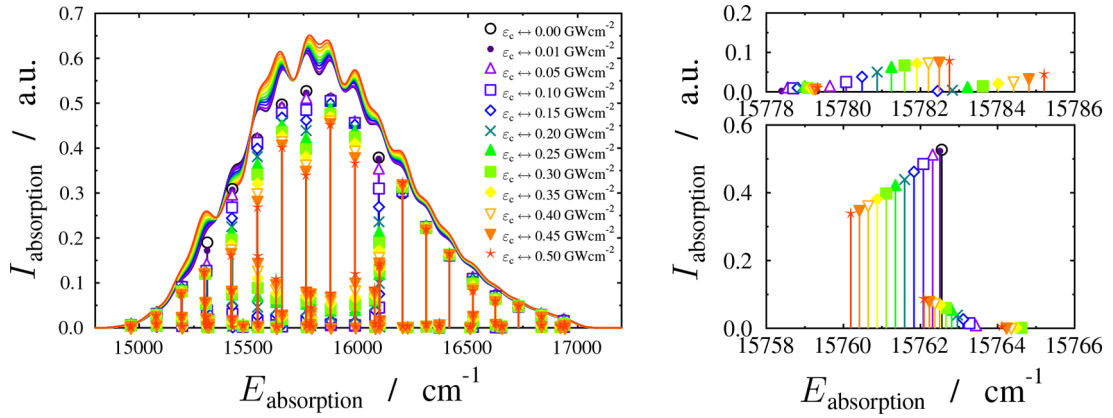

Figure 4. Field-dressed spectra obtained with different values of the light−matter coupling strengths for a cavity-mode wavelength of λ = 653 nm. Coupling strength values are indicated by the intensity of a classical light field giving a coupling strength equal to the one-photon coupling of the cavity; see eq 3. The envelope lines depict the spectra convolved with a Gaussian function having a standard deviation of σ = 50 cm^{-1}.

obtained by diagonalizing the Hamiltonian corresponding to eq 4 in the basis of the field-free rovibrational states.

Let us now compute the absorption spectrum with respect to a weak probe pulse, whose photon number is represented by the letter M. Using first-order time-dependent perturbation theory, the transition amplitude between two field-dressed states, induced by the weak probe pulse, can be expressed as[57,58]

$$\langle \Psi_i^{FD}|\langle M|\hat{\mathbf{d}}\hat{\mathbf{E}}|M'\rangle|\Psi_j^{FD}\rangle = \langle \Psi_i^{FD}|\hat{d}\ \cos(\theta)|\Psi_j^{FD}\rangle\langle M|\hat{E}|M'\rangle \tag{8}$$

In eq 8, the electric-field operator $\hat{E}$ stands for the weak probe pulse, and we assume that the probe pulse has a polarization axis identical to that of the cavity mode. Because $\hat{E}$ is proportional to the sum of a creation and an annihilation operator acting on $|M'\rangle$, eq 8 leads to the well-known result that the transition amplitude is nonzero only if $M = M' \pm 1$; that is, eq 8 accounts for single-photon absorption or stimulated emission.

The matrix element of the operator $\hat{d}\cos(\theta)$ between two field-dressed states of eq 7 gives

$$\begin{aligned}\langle \Psi_i^{FD}|\hat{d}\ \cos(\theta)|\Psi_j^{FD}\rangle &= \left(\sum_{J,\upsilon,\alpha,N} C^*_{i,\alpha\upsilon JN}\langle \alpha\upsilon J|\langle N|\right)\hat{d}\ \cos(\theta)\left(\sum_{J',\upsilon',\alpha',N'} C_{j,\alpha'\upsilon'J'N'}|\alpha'\upsilon'J'\rangle|N'\rangle\right)\\ &= \sum_{J,\upsilon,\alpha,N,J',\upsilon',\alpha',N'} C^*_{i,\alpha\upsilon JN}C_{j,\alpha'\upsilon'J'N'}\langle \alpha\upsilon J|\hat{d}\ \cos(\theta)|\alpha'\upsilon'J'\rangle\delta_{N,N'}\\ &= \sum_{J,\upsilon,J',\upsilon',N} C^*_{i,1\upsilon JN}C_{j,2\upsilon'J'N}\langle 1\upsilon J|\hat{d}\ \cos(\theta)|2\upsilon'J'\rangle + \sum_{J,\upsilon,J',\upsilon',N} C^*_{i,2\upsilon JN}C_{j,1\upsilon'J'N}\langle 2\upsilon J|\hat{d}\ \cos(\theta)|1\upsilon'J'\rangle\end{aligned} \tag{9}$$

In the last line of eq 9, the first (second) term represents transitions in which the first (second) electronic state contributes from the ith field-dressed state and the second (first) electronic state contributes from the jth field-dressed state. Assuming that the ith state is the initial state, the first term in the last line of eq 9 leads to the usual field-free absorption spectrum in the limit of the light−matter coupling going to zero. In all of the spectra shown in this study, we plot the absolute square of the transition amplitudes, as computed by eq 9, or their convolution with a Gaussian function.

We apply the theoretical framework developed in eqs 1−9 to the Na_2 molecule, for which the $V_1(R)$ and $V_2(R)$ PECs correspond to the $X^1\Sigma_g^+$ and the $A^1\Sigma_u^+$ electronic states, respectively. The PECs and the transition dipole are taken from refs 59 and 60, respectively.

In Figure 3 the employed PECs of Na_2 are shown, and some important physical processes are indicated as well. The main results of this study are conveniently depicted in Figures 4−6. Each figure will be discussed separately.

The left panel of Figure 3 shows PECs of Na_2 dressed with a different number of photons in the cavity radiation field as well as vibrational probability densities for direct-product states of the $|j\upsilon J\rangle|N\rangle$ form. As apparent from eq 4 and illustrated by the double-headed arrows in Figure 3, light−matter interaction can give rise to resonant $|1\ \upsilon\ J\rangle|N\rangle \leftrightarrow |2\ \upsilon'\ J \pm 1\rangle|N-1\rangle$ and nonresonant $|1\ \upsilon\ J\rangle|N\rangle \leftrightarrow |2\ \upsilon'\ J \pm 1\rangle|N+1\rangle$-type couplings, which lead to the formation of field-dressed states; see eq 7. The terms "resonant" and "nonresonant" indicate whether the direct-product states that are coupled are close in energy; see Figure 3. Naturally, resonant couplings are much more efficient in mixing the direct-product states than nonresonant couplings. For comparison, the right panel of Figure 3 shows the light-dressed PECs of Na_2 in a laser field.[24] Because nonresonant couplings are omitted in the usual Floquet description[61] of laser-light-dressed molecules, these couplings are not shown in the right panel of Figure 3. It is clear from Figure 3 that the absorption spectrum of field-dressed molecules should be considerably different for the cavity-dressed and laser-dressed cases. The most significant difference is that whereas in the cavity the ground state is primarily a field-free eigenstate in vacuum, which is only deformed at relatively large coupling strengths through nonresonant couplings, the laser-light-

DOI: 10.1021/acs.jpclett.8b02609
J. Phys. Chem. Lett. 2018, 9, 6215−6223

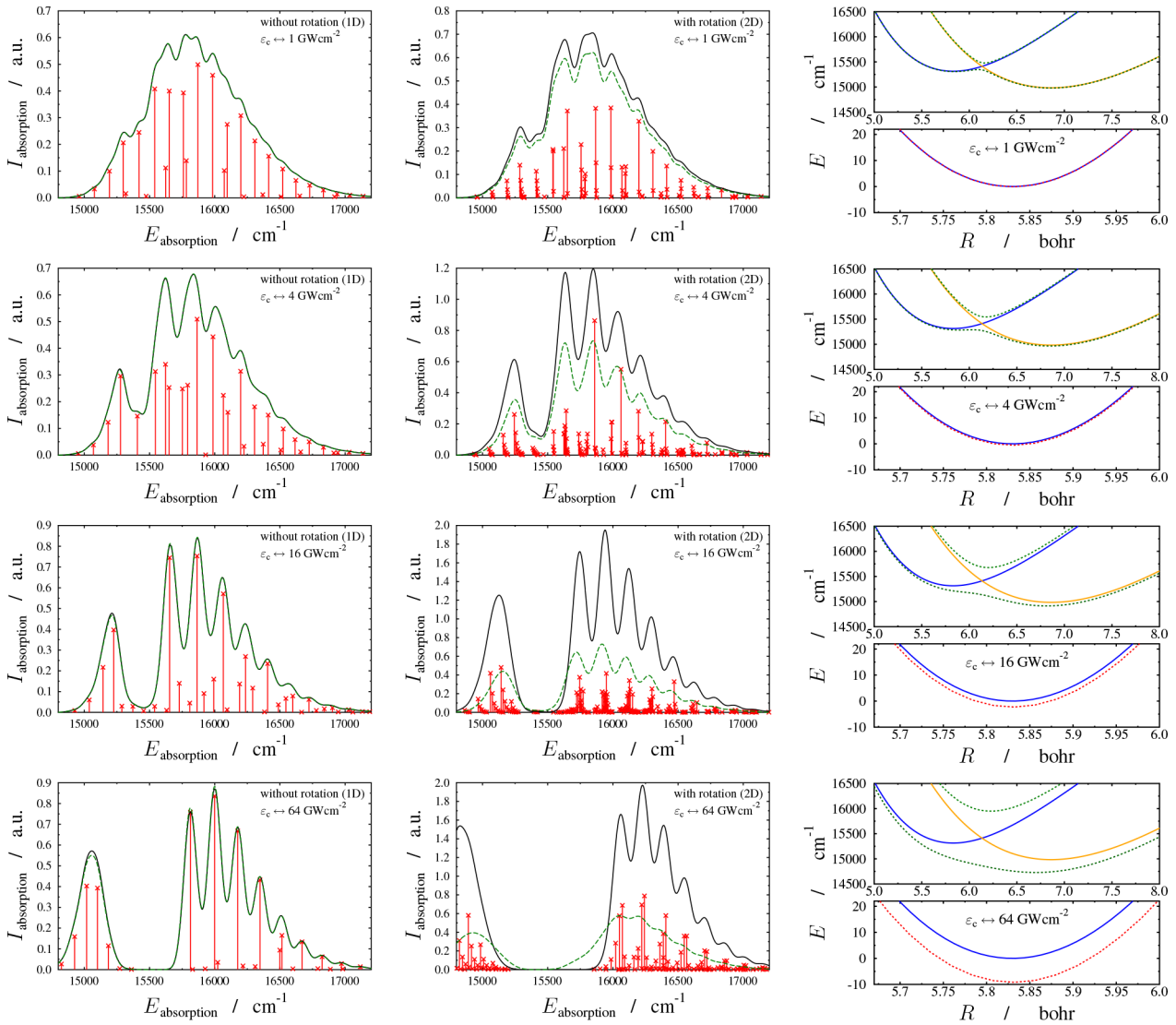

Figure 5. First two columns: field-dressed spectra obtained with different values of the light−matter coupling strengths for a cavity-mode wavelength of λ = 653 nm. Coupling strength values are indicated by the intensity of a classical light field giving a coupling strength equal to the one-photon coupling of the cavity; see eq 3. The envelope lines depict the spectra convoluted with a Gaussian function having a standard deviation of σ = 50 cm^{-1}. The labels "1D" and "2D" stand for vibration only and rovibrational calculations, defined by using J_{max} = 1 and J_{max} = 30, respectively. Solid and dashed lines correspond to calculations including or excluding the nonresonant couplings in the Hamiltonian, respectively; that is, the solid and dashed lines refer to using the upper left three-by-three or six-by-six block of the Hamiltonian in eq 4, respectively. Third column: diabatic and adiabatic PECs at different light−matter coupling strength values.

dressed state correlating to the field-free ground state contains a mixture of field-free eigenstates due to the strong resonant coupling in this case.

Figure 4 shows field-dressed spectra obtained with different values of the $\varepsilon_c = \sqrt{\hbar\omega_c/(\epsilon_0 V)}$ cavity one-photon field strength in the weak-coupling regime for a cavity-mode wavelength of λ = 653 nm. Although the light−matter coupling strength and the cavity-mode wavelength are not completely independent in a cavity (see eq 5), we treat them as independent parameters. This can be rationalized partially by eq 5, which shows that the coupling strength could be changed independently by changing the cavity volume while keeping the cavity length responsible for the considered cavity radiation mode fixed. The spectra in Figure 4 were computed assuming that the initial state is the ground state of the full system. The left panel of Figure 4 reflects features similar to those observed in the spectrum of Na_2 dressed by laser fields.[24] With increasing light−matter coupling, the overall intensity of the spectrum slightly increases at almost all wavenumbers, with some shoulder features becoming more pronounced in the spectrum envelope. In terms of spectroscopic nomenclature, such a phenomenon can be understood as an intensity-borrowing effect,[62−64] which arises from the field-induced couplings between field-free states.

On the other hand, the coupling-strength dependence of the spectrum envelope is completely absent if the spectra in Figure 4 are generated from computations in which the rotational motion is restricted by setting J_{max} = 1. Such a rotationally restricted model inherently lacks any signatures of a LICI, whose formation requires at least two nuclear degrees of freedom. Therefore, in terms of the adiabatic representation, the intensity borrowing effect visible in Figure 4 can be attributed to the nonadiabatic couplings of a LICI created by the quantized cavity radiation field.

DOI: 10.1021/acs.jpclett.8b02609
J. Phys. Chem. Lett. 2018, 9, 6215−6223

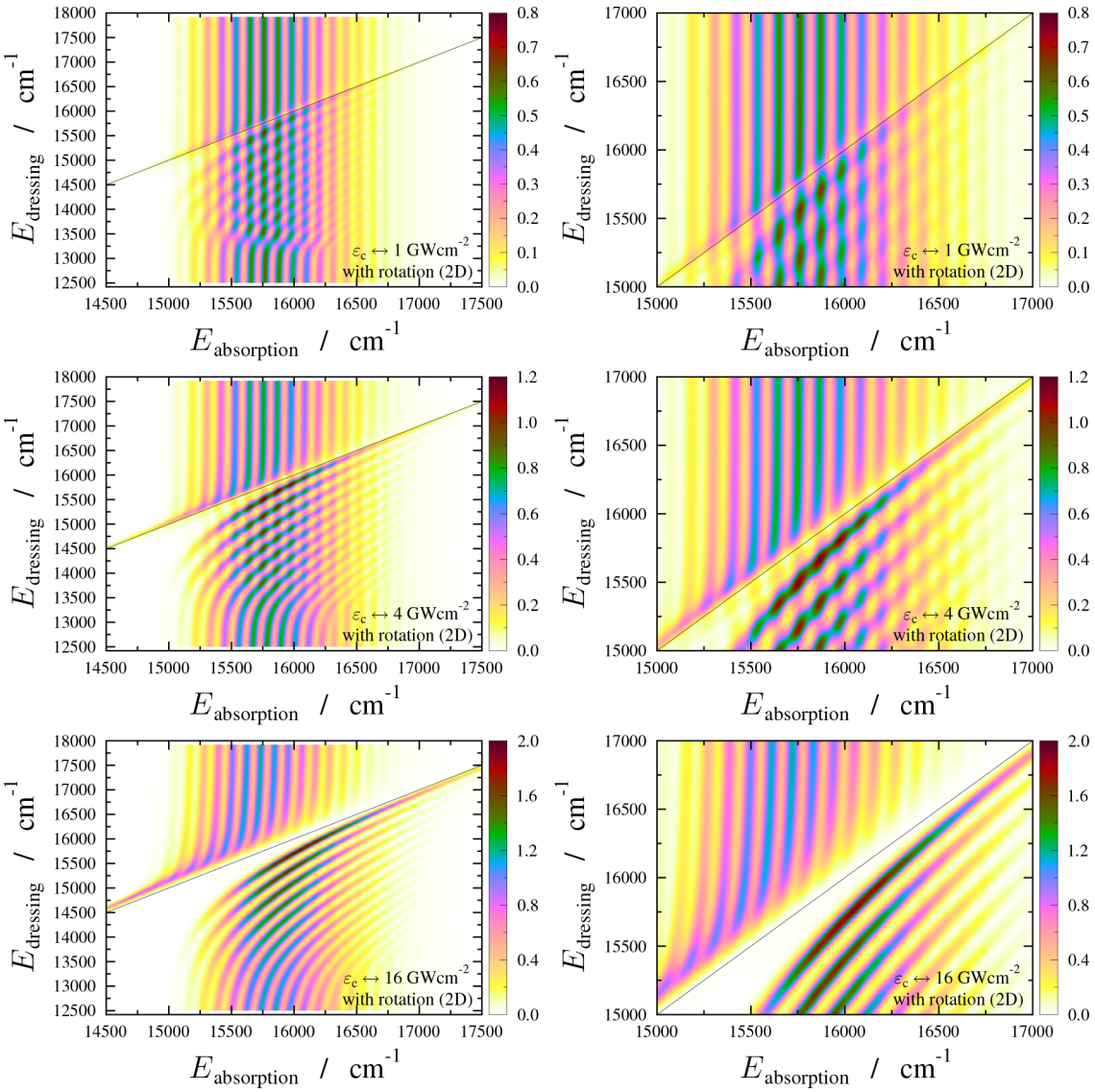

Figure 6. Dependence of the absorption spectrum on the $E_{dressing}$ wavenumber of the cavity mode, computed at three different coupling strengths and using eq 9. The λ = 653 nm wavelength used in previous figures stands for 15 314 cm^{-1}. Coupling strength values are indicated by the intensity of a classical light field giving a coupling strength equal to the one-photon coupling of the cavity; see eq 3. The spectrum is convoluted at each fixed cavity-mode wavelength with a Gaussian function having σ = 30 cm^{-1}. The thin black lines represent $E_{dressing}$ = $E_{absorption}$.

Inspection of individual transition lines in the spectra reveals that increasing the light−matter coupling strength can result in the splitting of existing peaks and the appearance of additional peaks, as shown in the two panels on the right side of Figure 4. The upper right panel of Figure 4 shows the progression of three peaks, corresponding to transitions from the initial state (essentially the $|1\ 0\ 0\rangle|0\rangle$ state) to field-dressed states primarily composed of the $|2\ 7\ 1\rangle|0\rangle$, $|2\ 7\ 3\rangle|0\rangle$, and $|2\ 7\ 5\rangle|0\rangle$ states, with $|1\ v\ J\rangle|1\rangle$-type states (J even) contributing as well. With increasing light−matter coupling strength these transitions are red-shifted, and they can be interpreted as originating from the field-free transition $|1\ 0\ 0\rangle \rightarrow |2\ 7\ 1\rangle$, which is split due to the mixing of $|2\ 7\ 1\rangle$ with other states through the resonant light−matter coupling with the cavity mode. The lower right panel of Figure 4 shows the progression of three peaks, which do not arise from the splitting of an existing field-free peak but appear as new peaks. These transitions are blue-shifted with increasing light−matter coupling strength, and they occur between the initial state (essentially the $|1\ 0\ 0\rangle|0\rangle$ state) and field-dressed states primarily composed of the $|1\ 3\ 0\rangle|1\rangle$, $|1\ 3\ 2\rangle|1\rangle$, and $|1\ 3\ 4\rangle|1\rangle$ states. Such transitions are forbidden in the zero light−matter coupling limit; however, they become visible as the light−matter coupling with the cavity mode contaminates the $|1\ 3\ J\rangle|1\rangle$ states with $|2\ v\ 1\rangle|0\rangle$-type states, to which the initial state has allowed transitions.

In Figure 5 field-dressed spectra obtained with light−matter coupling strengths ranging from the weak to the ultrastrong coupling regimes are shown for a cavity-mode wavelength of λ = 653 nm. Because in current experiments the rotational structure cannot be resolved, from now on we focus on the behavior of the spectrum envelopes. The spectra labeled "1D" in Figure 5 were obtained with a model having restricted rotational motion (J_{max} = 1). The results labeled "2D" fully account for rotations as well as vibrations and therefore incorporate the effects of a LICI on the spectrum.

DOI: 10.1021/acs.jpclett.8b02609
J. Phys. Chem. Lett. 2018, 9, 6215−6223

By comparing the "1D" and "2D" spectrum envelopes in Figure 5, it is apparent that there is a significant increase in absorption for the "2D" case. As discussed below, this is primarily due to nonresonant light−matter couplings between $|1\ 0\ J\rangle|0\rangle$- and $|2\ v'\ J \pm 1\rangle|1\rangle$-type states and partially to the intensity-borrowing effect induced by the nonadiabatic couplings of the LICI.

Figure 5 also shows field-dressed PECs in the diabatic and adiabatic representations. As the coupling strength increases, two separate polariton surfaces are formed due to resonant light−matter couplings, and the absorption spectrum splits into two distinct groups of peaks, corresponding to transitions onto the two polariton states. At the largest coupling strength, nonresonant light−matter couplings lead to a slight modification of the ground-state PEC, indicating that the ultrastrong coupling regime has been reached.

Even at the largest coupling strength investigated in this study the modification of the ground-state PEC is on the order of a few tens of cm^{-1}, which is far too small to influence chemical reactivity by modifying the vibrational motion along the PEC. Nonetheless, interestingly, nonresonant couplings seem to have an impact on the spectrum at much smaller coupling strengths than those required for a significant modification of the ground-state PEC. The spectrum envelopes depicted with continuous and dashed lines in Figure 5 indicate whether spectra were computed by using the upper left three-by-three block of the Hamiltonian in eq 4 or a six-by-six block, respectively. The deviation between these two types of spectra represents the effect of nonresonant couplings because the $\hat{T} + V_2(R) + \hbar\omega_c$ term and its couplings with $\hat{T} + V_1(R)$ are absent if only the upper left three-by-three block of eq 4 is used. The plots in Figure 5 clearly demonstrate that in the vibration-only "1D" case nonresonant couplings have no visible impact on the spectrum; however, for the "2D" case, in which rotations are accounted for, nonresonant couplings lead to a visible increase in the absorption signal even at the lowest coupling strengths shown. The physical origin of the increase in absorption is the contamination of the $|1\ 0\ 0\rangle|0\rangle$ ground state with the $|1\ 0\ 2\rangle|0\rangle$, $|1\ 0\ 4\rangle|0\rangle$, ... states, which allows for transitions onto the $J = 3, 5, \ldots$ components of the rovibronic states in the excited polariton manifold. These results indicate that the effects of nonresonant couplings cannot be described in a vibration-only model, and if one wishes to obtain meaningful simulation results for coupling strengths reaching or exceeding those shown in Figure 5, then it is necessary to properly account for molecular rotations.

Figure 6 shows the cavity-mode wavenumber dependence of the field-dressed spectrum obtained at the ε_c cavity one-photon field strengths of 0.844×10^{-4}, 1.688×10^{-4}, and 3.376×10^{-4} (in a.u.), corresponding to classical field intensities of 1, 4, and 16 GW cm^{-2}, respectively. It can be concluded from Figure 6 that, as expected, the field-dressed spectrum changes with the cavity-mode wavelength. Furthermore, the cavity-mode wavelength dependence of the spectrum shows qualitative features considerably different from the dressing-field wavelength dependence of the spectrum when Na_2 is dressed by medium-intensity laser fields,[24] as one might expect from Figure 3.

For all coupling strengths shown in Figure 6, at large dressing-field photon energies, that is, those exceeding 17 000 cm^{-1} or so, the spectra resemble the field-free spectrum, depicting ∼20 lines corresponding to transitions to $|2\ v\ 1\rangle|0\rangle$-type states. This is expected, as for such large photon energies the $V_1(R) + \hbar\omega_c$ PEC crosses the $V_2(R)$ PEC at short internuclear distances, and the $V_2(R)$ PEC remains unperturbed in the Frank−Condon region. As the photon energy of the dressing field is lowered and the crossing of the $V_1(R) + \hbar\omega_c$ and $V_2(R)$ PECs approaches the Frank−Condon region, the spectrum becomes perturbed.

In the top row of Figure 6, a decrease can be seen in the spectrum line intensities along diagonal lines in the plots, forming island-type features. Focusing on a specific vibrational state on $V_2(R)$, corresponding to a vertical line in the plots, a decrease in the spectrum intensity occurs when this vibrational state becomes resonant with one of the $|1\ v\ J\rangle|1\rangle$ states. Because of the resonance, a strong mixing occurs between the $|1\ v\ J\rangle|1\rangle$- and $|2\ v'\ J'\rangle|0\rangle$-type states, which leads to a decrease in the transition amplitude from the ground state. Nonetheless, when the mixing of the states is not as efficient as in the resonant case, that is, at the island-type features on the plots, an increase can be seen in the spectrum intensities with respect to the field-free case.

As depicted in the middle and bottom rows of Figure 6, when the coupling strength is increased, the picture of a "perturbed spectrum" gradually changes into the picture of two distinct spectra corresponding to the two polariton surfaces, in accordance with Figure 5. The dressing-field wavenumber dependence of the spectrum in the bottom row of Figure 6 can easily be understood in terms of the wavenumber dependence of the polariton surfaces depicted in the rightmost column of Figure 5.

To summarize, we investigated the rovibronic spectrum of homonuclear diatomic molecules dressed by the quantized radiation field of an optical cavity. The formation of light-induced conical intersections induced by the quantized radiation field is shown for the first time by identifying the robust light-induced nonadiabatic effects in the spectrum. The coupling strength and the cavity-mode-wavelength dependence of the field-dressed spectrum is also investigated from the weak to the ultrastrong coupling regimes. The formation of polariton states in the strong coupling regime is demonstrated, and it is shown how nonresonant couplings lead to an increased absorption in the field-dressed spectrum even before the ultrastrong coupling regime is reached. The strong modification in the rovibronic photoabsorption spectrum via increasing coupling strength carries the changes induced in both the ground state and the upper and lower polaritonic states. Whereas the formation of the polaritonic states qualitatively changes the spectrum, the much less pronounced changes in the ground state primarily affect the peak intensities. The numerical results obtained for the Na_2 test system also demonstrate that the additional degree of freedom (which is the rotation in the present diatomic situation) plays a crucial role in the light-induced nonadiabatic processes as well as in the efficiency of nonresonant couplings. Therefore, in experimental scenarios when molecular rotations can proceed in the cavity, the spectrum is expected to deviate from the rotationally hindered case, and properly accounting for the rotational degrees of freedom in the complementing simulations is mandatory for obtaining reliable results.

We hope that our findings will stimulate the extension of the theory for the proper description of polyatomic molecules. Nonetheless, it did not escape our attention that there is much potential in studying light-induced conical

DOI: 10.1021/acs.jpclett.8b02609
J. Phys. Chem. Lett. 2018, 9, 6215−6223

intersections in polyatomic molecules in the cavity without rotations because there are many nuclear degrees of freedom to form such intersections that can also be used to selectively manipulate certain chemical and physical properties.

AUTHOR INFORMATION

Corresponding Authors

*T.Sz.: E-mail: tamas821@caesar.elte.hu.
*Á.V.: E-mail: vibok@phys.unideb.hu.

ORCID

Tamás Szidarovszky: 0000-0003-0878-5212
Attila G. Császár: 0000-0001-5640-191X
Ágnes Vibók: 0000-0001-6821-9525

Notes

The authors declare no competing financial interest.

ACKNOWLEDGMENTS

This research was supported by the EU-funded Hungarian grant EFOP-3.6.2-16-2017-00005 and by the Deutsche Forschungsgemeinschaft (Project ID CE10/50-3). We are grateful to NKFIH for support (grant nos. PD124623, K119658, and K128396). We thank Péter Domokos and Markus Kowalewski for fruitful discussions.

REFERENCES

(1) Brabec, T.; Krausz, F. Intense Few-Cycle Laser Fields: Frontiers of Nonlinear Optics. *Rev. Mod. Phys.* **2000**, *72*, 545−591.
(2) Krausz, F.; Ivanov, M. Attosecond Physics. *Rev. Mod. Phys.* **2009**, *81*, 163−234.
(3) Kruchinin, S. Y.; Krausz, F.; Yakovlev, V. S. Colloquium: Strong-Field Phenomena in Periodic Systems. *Rev. Mod. Phys.* **2018**, *90*, 021002.
(4) Krause, J. L.; Schafer, K. J.; Kulander, K. C. High-Order Harmonic Generation from Atoms and Ions in the High Intensity Regime. *Phys. Rev. Lett.* **1992**, *68*, 3535−3538.
(5) Lewenstein, M.; Balcou, P.; Ivanov, M. Y.; L'Huillier, A.; Corkum, P. B. Theory of High-Harmonic Generation by Low-Frequency Laser Fields. *Phys. Rev. A: At., Mol., Opt. Phys.* **1994**, *49*, 2117−2132.
(6) Schafer, K. J.; Yang, B.; DiMauro, L. F.; Kulander, K. C. Above Threshold Ionization Beyond the High Harmonic Cutoff. *Phys. Rev. Lett.* **1993**, *70*, 1599−1602.
(7) Bandrauk, A. D.; Sink, M. L. Laser Induced Preassociation in the Presence of Natural Predissociation. *Chem. Phys. Lett.* **1978**, *57*, 569−572.
(8) Bandrauk, A. D.; Atabek, O. Semiclassical Methods in Multiphoton Diatomic Spectroscopy: Beyond Perturbation Theory. *J. Phys. Chem.* **1987**, *91*, 6469−6478.
(9) Aubanel, E. E.; Gauthier, J.-M.; Bandrauk, A. D. Molecular Stabilization and Angular Distribution in Photodissociation of H_2^+ in Intense Laser Fields. *Phys. Rev. A: At., Mol., Opt. Phys.* **1993**, *48*, 2145−2152.
(10) Bandrauk, A. D.; Aubanel, E. E.; Gauthier, J. M. *Molecules in Laser Fields*; Marcel Dekker: New York, 1994.
(11) Bucksbaum, P. H.; Zavriyev, A.; Muller, H. G.; Schumacher, D. W. Softening of the H_2^+ Molecular Bond in Intense Laser Fields. *Phys. Rev. Lett.* **1990**, *64*, 1883−1886.
(12) Zavriyev, A.; Bucksbaum, P. H.; Muller, H. G.; Schumacher, D. W. Ionization and Dissociation of H_2 in Intense Laser Fields at 1.064 micron, 532 nm, and 355 nm. *Phys. Rev. A: At., Mol., Opt. Phys.* **1990**, *42*, 5500−5513.
(13) Zavriyev, A.; Bucksbaum, P. H.; Squier, J.; Saline, F. Light-Induced Vibrational Structure in H_2^+ and D_2^+ in Intense Laser Fields. *Phys. Rev. Lett.* **1993**, *70*, 1077−1080.
(14) Halász, G. J.; Vibók, Á.; Šindelka, M.; Moiseyev, N.; Cederbaum, L. S. Conical Intersections Induced by Light: Berry Phase and Wavepacket Dynamics. *J. Phys. B: At., Mol. Opt. Phys.* **2011**, *44*, 175102.
(15) Halász, G. J.; Šindelka, M.; Moiseyev, N.; Cederbaum, L. S.; Vibók, Á. Light-Induced Conical Intersections: Topological Phase,Wave Packet Dynamics, and Molecular Alignment. *J. Phys. Chem. A* **2012**, *116*, 2636−2643.
(16) Halász, G. J.; Csehi, A.; Vibók, Á.; Cederbaum, L. S. Influence of Light-Induced Conical Intersection on the Photodissociation Dynamics of D_2^+ Starting from Individual Vibrational Levels. *J. Phys. Chem. A* **2014**, *118*, 11908−11915.
(17) Csehi, A.; Halász, G. J.; Cederbaum, L. S.; Vibók, Á. Towards Controlling the Dissociation Probability by Light-Induced Conical Intersections. *Faraday Discuss.* **2016**, *194*, 479−493.
(18) Halász, G. J.; Vibók, Á.; Cederbaum, L. S. Direct Signature of Light-Induced Conical Intersections in Diatomics. *J. Phys. Chem. Lett.* **2015**, *6*, 348−354.
(19) Csehi, A.; Halász, G. J.; Cederbaum, L. S.; Vibók, Á. Competition between Light-Induced and Intrinsic Nonadiabatic Phenomena in Diatomics. *J. Phys. Chem. Lett.* **2017**, *8*, 1624−1630.
(20) Shu, C. C.; Yuan, K. J.; Dong, D.; Petersen, I. R.; Bandrauk, A. D. Identifying Strong-Field Effects in Indirect Photofragmentation. *J. Phys. Chem. Lett.* **2017**, *8*, 1−6.
(21) Šindelka, M.; Moiseyev, N.; Cederbaum, L. S. Strong Impact of Light-Induced Conical Intersections on the Spectrum of Diatomic Molecules. *J. Phys. B: At., Mol. Opt. Phys.* **2011**, *44*, 045603.
(22) Demekhin, P. V.; Cederbaum, L. S. Light-Induced Conical Intersections in Polyatomic Molecules: General Theory, Strategies of Exploitation, and Application. *J. Chem. Phys.* **2013**, *139*, 154314.
(23) Conical intersections (CIs) are geometries where two electronic states of a molecule share the same energy, providing a very efficient channel for nonradiative relaxation processes to the ground state on an ultrafast time scale. For CIs to be formed in a molecular system, one needs two independent degrees of freedom, which constitute the space in which the CIs can exist. Therefore, CIs between different electronic states can only occur for molecules with at least three atoms. For a diatomic molecule, which has only one vibrational degree of freedom, it is not possible for two electronic states of the same symmetry to become degenerate, as required by the well-known noncrossing rule. However, this statement is true only in free space.
(24) Szidarovszky, T.; Halász, G. J.; Császár, A. G.; Cederbaum, L. S.; Vibók, Á. Direct Signatures of Light-Induced Conical Intersections on the Field-Dressed Spectrum of Na_2. *J. Phys. Chem. Lett.* **2018**, *9*, 2739−2745.
(25) Ebbesen, T. W. Hybrid Light-Matter States in a Molecular and Material Science Perspective. *Acc. Chem. Res.* **2016**, *49*, 2403−2412.
(26) Flick, J.; Ruggenthaler, M.; Appel, H.; Rubio, A. Atoms and Molecules in Cavities, from Weak to Strong Coupling in Quantum-Electrodynamics (QED) Chemistry. *Proc. Natl. Acad. Sci. U. S. A.* **2017**, *114*, 3026−3034.
(27) Feist, J.; Galego, J.; Garcia-Vidal, F. J. Polaritonic Chemistry with Organic Molecules. *ACS Photonics* **2018**, *5*, 205−216.
(28) Ribeiro, R. F.; Martínez-Martínez, L. A.; Du, M.; Campos-Gonzalez-Angulo, J.; Yuen-Zhou, J. Polariton Chemistry: Controlling Molecular Dynamics with Optical Cavities. *Chem. Sci.* **2018**, *9*, 6325−6339.
(29) Flick, J.; Rivera, N.; Narang, P. Strong Light-Matter Coupling in Quantum Chemistry and Quantum Photonics. *Nanophotonics* **2018**, *7*, 1479−1501.
(30) Chikkaraddy, R.; de Nijs, B.; Benz, F.; Barrow, S. J.; Scherman, O. A.; Rosta, E.; Demetriadou, A.; Fox, P.; Hess, O.; Baumberg, J. J. Single-Molecule Strong Coupling at Room Temperature in Plasmonic Nanocavities. *Nature* **2016**, *535*, 127−130.

DOI: 10.1021/acs.jpclett.8b02609
J. Phys. Chem. Lett. 2018, 9, 6215−6223

(31) Ruggenthaler, M.; Tancogne-Dejean, N.; Flick, J.; Appel, H.; Rubio, A. From a Quantum-Electrodynamical Light-Matter Description to Novel Spectroscopies. *Nat. Rev. Chem.* **2018**, *2*, 0118.
(32) Vukics, A.; Grießer, T.; Domokos, P. Fundamental Limitation of Ultrastrong Coupling Between Light and Atoms. *Phys. Rev. A: At., Mol., Opt. Phys.* **2015**, *92*, No. 043835.
(33) Hutchison, J. A.; Schwartz, T.; Genet, C.; Devaux, E.; Ebbesen, T. W. Modifying Chemical Landscapes by Coupling to Vacuum Fields. *Angew. Chem., Int. Ed.* **2012**, *51*, 1592−1596.
(34) Schwartz, T.; Hutchison, J. A.; Léonard, J.; Genet, C.; Haacke, S.; Ebbesen, T. W. Polariton Dynamics under Strong Light-Molecule Coupling. *ChemPhysChem* **2013**, *14*, 125−131.
(35) George, J.; Wang, S.; Chervy, T.; Canaguier-Durand, A.; Schaeffer, G.; Lehn, J.-M.; Hutchison, J. A.; Genet, C.; Ebbesen, T. W. Ultra-Strong Coupling of Molecular Materials: Spectroscopy and Dynamics. *Faraday Discuss.* **2015**, *178*, 281−294.
(36) Zhong, X.; Chervy, T.; Wang, S.; George, J.; Thomas, A.; Hutchison, J. A.; Devaux, E.; Genet, C.; Ebbesen, T. W. Non-Radiative Energy Transfer Mediated by Hybrid Light-Matter States. *Angew. Chem., Int. Ed.* **2016**, *55*, 6202−6206.
(37) Muallem, M.; Palatnik, A.; Nessim, G. D.; Tischler, Y. R. Strong Light-Matter Coupling and Hybridization of Molecular Vibrations in a Low-Loss Infrared Microcavity. *J. Phys. Chem. Lett.* **2016**, *7*, 2002−2008.
(38) Thomas, A.; George, J.; Shalabney, A.; Dryzhakov, M.; Varma, S. J.; Moran, J.; Chervy, T.; Zhong, X.; Devaux, E.; Genet, C.; et al. Ground-State Chemical Reactivity under Vibrational Coupling to the Vacuum Electromagnetic Field. *Angew. Chem., Int. Ed.* **2016**, *55*, 11462−11466.
(39) Galego, J.; Garcia-Vidal, F. J.; Feist, J. Cavity-Induced Modifications of Molecular Structure in the Strong-Coupling Regime. *Phys. Rev. X* **2015**, *5*, 1−14.
(40) Herrera, F.; Spano, F. C. Cavity-Controlled Chemistry in Molecular Ensembles. *Phys. Rev. Lett.* **2016**, *116*, 238301.
(41) Galego, J.; Garcia-Vidal, F. J.; Feist, J. Suppressing Photochemical Reactions with Quantized Light Fields. *Nat. Commun.* **2016**, *7*, 13841.
(42) Kowalewski, M.; Bennett, K.; Mukamel, S. Cavity Femtochemistry: Manipulating Nonadiabatic Dynamics at Avoided Crossings. *J. Phys. Chem. Lett.* **2016**, *7*, 2050−2054.
(43) Luk, H. L.; Feist, J.; Toppari, J. J.; Groenhof, G. Multiscale Molecular Dynamics Simulations of Polaritonic Chemistry. *J. Chem. Theory Comput.* **2017**, *13*, 4324−4335.
(44) Herrera, F.; Spano, F. C. Dark Vibronic Polaritons and the Spectroscopy of Organic Microcavities. *Phys. Rev. Lett.* **2017**, *118*, 223601.
(45) Galego, J.; Garcia-Vidal, F. J.; Feist, J. Many-Molecule Reaction Triggered by a Single Photon in Polaritonic Chemistry. *Phys. Rev. Lett.* **2017**, *119*, 136001.
(46) Flick, J.; Appel, H.; Ruggenthaler, M.; Rubio, A. Cavity Born−Oppenheimer Approximation for Correlated Electron−Nuclear-Photon Systems. *J. Chem. Theory Comput.* **2017**, *13*, 1616−1625.
(47) Triana, J. F.; Peláez, D.; Sanz-vicario, J. L. Entangled Photonic-Nuclear Molecular Dynamics of LiF in Quantum Optical Cavities. *J. Phys. Chem. A* **2018**, *122*, 2266−2278.
(48) Vendrell, O. Coherent Dynamics in Cavity Femtochemistry: Application of the Multi- Configuration Time-Dependent Hartree Method. *Chem. Phys.* **2018**, *509*, 55−65.
(49) Zeb, M. A.; Kirton, P. G.; Keeling, J. Exact States and Spectra of Vibrationally Dressed Polaritons. *ACS Photonics* **2018**, *5*, 249−257.
(50) Herrera, F.; Spano, F. C. Theory of Nanoscale Organic Cavities: The Essential Role of Vibration-Photon Dressed States. *ACS Photonics* **2018**, *5*, 65−79.
(51) Martínez-Martínez, L. A.; Ribeiro, R. F.; Campos-González-Angulo, J.; Yuen-Zhou, J. Can Ultrastrong Coupling Change Ground-State Chemical Reactions? *ACS Photonics* **2018**, *5*, 167−176.
(52) Ciuti, C.; Carusotto, I. Input-Output Theory of Cavities in the Ultrastrong Coupling Regime: The Case of Time-Independent Cavity Parameters. *Phys. Rev. A: At., Mol., Opt. Phys.* **2006**, *74*, No. 033811.
(53) Anappara, A. A.; De Liberato, S.; Tredicucci, A.; Ciuti, C.; Biasiol, G.; Sorba, L.; Beltram, F. Signatures of the Ultrastrong Light-Matter Coupling Regime. *Phys. Rev. B: Condens. Matter Mater. Phys.* **2009**, *79*, 201303.
(54) Born, M.; Oppenheimer, J. R. Zur Quantentheorie der Molekeln. *Ann. Phys.* **1927**, *389*, 457.
(55) Born, M.; Huang, K. *Dynamical Theory of Crystal Lattices*; Oxford University Press: New York, 1954.
(56) Bunker, P. R.; Jensen, P. *Molecular Symmetry and Spectroscopy*; NRC Research Press: Ottawa, Ontario, 1998.
(57) Cohen-Tannoudji, C.; Dupont-Roc, J.; Grynberg, G. *Atom-Photon Interactions: Basic Processes and Applications*; Wiley-VCH Verlag GmbH and Co.: Weinheim, Germany, 2004.
(58) Jaynes, E. T.; Cummings, F. W. Comparison of Quantum and Semiclassical Radiation Theories with Application to the Beam Maser. *Proc. IEEE* **1963**, *51*, 89−109.
(59) Magnier, S.; Millié, P.; Dulieu, O.; Masnou-Seeuws, F. Potential Curves for the Ground and Excited States of the Na_2 Molecule up to the (3*s*+5*p*) Dissociation Limit: Results of Two Different Effective Potential Calculations. *J. Chem. Phys.* **1993**, *98*, 7113−7125.
(60) Zemke, W. T.; Verma, K. K.; Vu, T.; Stwalley, W. C. An Investigation of Radiative Transition Probabilities for the $A^1\Sigma_u^+$-$X^1\Sigma_g^+$ Bands of Na2. *J. Mol. Spectrosc.* **1981**, *85*, 150−176.
(61) Chu, S.-I.; Telnov, D. A. Beyond the Floquet Theorem: Generalized Floquet Formalisms and Quasienergy Methods for Atomic and Molecular Multiphoton Processes in Intense Laser Fields. *Phys. Rep.* **2004**, *390*, 1−131.
(62) Köuppel, H.; Domcke, W.; Cederbaum, L. S. Multimode Molecular Dynamics Beyond the Born-Oppenheimer Approximation. *Adv. Chem. Phys.* **2007**, *57*, 59−246.
(63) Worth, G. A.; Cederbaum, L. S. Beyond Born-Oppenheimer: Molecular Dynamics Through a Conical Intersection. *Annu. Rev. Phys. Chem.* **2004**, *55*, 127−158.
(64) Domcke, W.; Yarkony, D. R. Role of Conical Intersections in Molecular Spectroscopy and Photoinduced Chemical Dynamics. *Annu. Rev. Phys. Chem.* **2012**, *63*, 325.

DOI: 10.1021/acs.jpclett.8b02609
J. Phys. Chem. Lett. 2018, 9, 6215−6223